

Silole-Containing Poly(silylenevinylene)s: Synthesis, Characterization, Aggregation-Enhanced Emission, and Explosive Detection

Zujin Zhao,¹ Tao Jiang,^{1,2} Yanju Guo,¹ Liyuan Ding,¹ Bairong He,¹ Zhengfeng Chang,¹ Jacky W. Y. Lam,² Jianzhao Liu,² Carrie Y. K. Chan,² Ping Lu,³ Liwen Xu,⁴ Huayu Qiu,^{1,4} Ben Zhong Tang²

¹College of Material, Chemistry and Chemical Engineering, Hangzhou Normal University, Hangzhou 310036, China

²Department of Chemistry and State Key Laboratory of Molecular Neuroscience, The Hong Kong University of Science and Technology, Clear Water Bay, Kowloon, Hong Kong, China

³State Key Laboratory of Supramolecular Structure and Materials, Jilin University, Changchun 130012, China

⁴Key Laboratory of Organosilicon Chemistry and Material Technology of Ministry of Education, Hangzhou Normal University, Hangzhou 310012, China

Correspondence to: H. Y. Qiu (E-mail: huayuqiu@gmail.com) or B. Z. Tang (E-mail: tangbenz@ust.hk)

Received 3 January 2012; accepted 9 February 2012; published online 13 March 2012

DOI: 10.1002/pola.26006

ABSTRACT: Hydrosilylation polymerizations of 1,1-dimethyl-2,5-bis(4-ethynylphenyl)-3,4-diphenylsilole with aromatic silylhydrides including 1,4-bis(dimethylsilyl)benzene, 4,4'-bis(dimethylsilyl)biphenyl, 2,5-bis(dimethylsilyl)thiophene, and 2,7-bis(dimethylsilyl)-9,9-dihexylfluorene in the presence of Rh(PPh₃)₃Cl catalyst in refluxed tetrahydrofuran afford a series of silole-containing poly(silylenevinylene)s. Under optimum condition, the alkyne polyhydrosilylation reactions progress efficiently and regioselectively, yielding polymers with high molecular weights (M_w up to 95,300) and good stereoregularity (E content close to 99%) in high yields (up to 92%). The polymers are processable and thermally stable, with high decomposition temperatures in the range of 420–449 °C corresponding to 5% weight loss. They are weakly fluores-

cent in the solution state but become emissive in the aggregate and film states, demonstrating their aggregation-enhanced emission characteristics. The explosive sensing capabilities of the polymers are examined in both solution and aggregate states. The emissions of the polymers aggregates in aqueous mixture are quenched more efficiently by picric acid in an exponential pattern with high quenching constants (up to 27,949 L mol⁻¹), suggesting that the polymers aggregates are sensitive chemosensors for explosive detection. © 2012 Wiley Periodicals, Inc. *J Polym Sci Part A: Polym Chem* 50: 2265–2274, 2012

KEYWORDS: aggregation-enhanced emission; explosive detection; fluorescence; heteroatom-containing polymers; synthesis

INTRODUCTION Siloles (silacyclopentadienes) are a group of silicon-containing five-membered cyclic dienes, which have attracted considerable research interests due to their unique electronic properties and potential high-technological applications. The effective interactions of the σ^* orbital of the exocyclic bonds on the silicon atom and the π^* orbital of the butadiene moiety result in low-lying lowest unoccupied molecular orbital of siloles, and thus endow them with high electron acceptability and fast electron mobility.¹ Recently, researchers found that a series of substituted propeller-like siloles that are nonfluorescent in solutions fluoresce strongly in aggregates or in solid films. Such a novel phenomenon coined as aggregation-induced emission (AIE)^{2,3} is exactly opposite to the emission behaviors of most conventional dyes, whose emissions become weak by aggregation formation. All these intriguing features have enabled siloles to find

applications in electron transport and/or light-emitting materials,⁴ solar cells,⁵ fluorescent bioprobes,⁶ and chemosensors.⁷

Currently, many efforts are made to create efficient functional materials for the rapid detection of nitroaromatic explosives, such as trinitrotoluene (TNT) and 2,4,6-trinitrophenol (picric acid, PA), which is of significant importance concerning the increasingly serious public security threats and environmental pollution problems across the globe. Fluorescent-conjugated polymers (FCP) have been introduced as low cost, robust materials for the detection of explosives vapors and particles.⁸ Swager et al. demonstrated that FCPs are superior in explosive detections to low-molecular-weight compounds.⁹ The fast exciton migration along the conjugated backbones provides an amplifying response to analytes, for the interaction of an analyte molecule at any position along

Additional Supporting Information may be found in the online version of this article.

© 2012 Wiley Periodicals, Inc.

the polymer chain is communicated throughout the conjugation system. However, the aggregation of the polymer backbones built with conventional chromophores often quenches the light emission, and thus undermines the sensing performance.

In an effort to create polymeric fluorescent chemosensors that can function efficiently in the aggregate state, we introduced AIE units, such as silole and tetraphenylethene (TPE) into the linear and hyperbranched polymers by metathesis, click, coupling, and cyclotrimerization polymerizations using acetylenes as building blocks.¹⁰ All of these polymers possess good solubility in common organic solvents and enjoy high thermal stability. The results show that incorporation of AIE-active monomers into polymers can solve the problem of such notorious aggregation-caused quenching (ACQ). The aggregates of the polymers containing AIE units emit more efficiently than individually dispersive species in the solution state. They outperform fluorescent polymers constructed by conventional chromophores in explosive detection. A super-amplification effect is usually observed from aggregates of AIE-active polymers: the quenching efficiency is greatly increased in a nonlinear fashion with increasing quencher concentration.^{10(g),11}

Hydrosilylation reactions between alkynes and silylhydrides catalyzed by various transition metals are well-established approaches to construct vinyl silane derivatives.¹² The reactions have been exploited in the preparation of linear and hyperbranched poly(silylenevinylene)s bearing functional groups as well. The polymers with silicon atoms may exhibit unique $\sigma^*-\pi$ delocalization along the polymer backbone due to the interaction of the σ^* orbitals of the silicon atoms and the π orbitals of the carbon-vinylene bonds.¹³ These polymers show potential applications as photoresists, cross-linkable prepolymers, ceramic precursors, electron-transporting materials, optoelectronic materials, and particularly, fluorescent chemosensors. Trogler et al. introduced siloles through the 1,1-positions of the metalole ring into a series of silylvinyl polymers by facile hydrosilylation polymerization of 2,3,4,5-tetraphenylsiloles with diynes. Their emissive nanoaggregates have shown promising application for the detection of a wide range of explosive particles.¹⁴ To further explore efficient polymeric organosilicon materials for explosive detection, in this article, we wish to report a series of silole-containing $\sigma^*-\pi$ -conjugated polymers, which are synthesized by hydrosilylation polymerizations of 2,5-bis(4-ethynylphenyl)-1,1-dimethyl-3,4-diphenylsilole with various aromatic silylhydrides. Their photophysical properties and applications for the explosive detection are presented.

EXPERIMENTAL

Materials and Instrumentations

Tetrahydrofuran (THF) was distilled under normal pressure from sodium benzophenone ketyl under nitrogen immediately before use. All the solvents of high purities were used without further purification. All the chemicals were purchased from Aldrich and used as received. Chlorotris(triphenylphosphine)rhodium(I) was synthesized following the liter-

ature method.¹⁵ The aromatic silylhydrides **1–4** were prepared by a modified method according to literature.¹⁶ 1,1-Dimethyl-2,5-bis(4-ethynylphenyl)-3,4-diphenylsilole (**5**)^{10(g)} was synthesized by our published method. IR spectra were recorded on a Perkin-Elmer 16 PC FTIR spectrophotometer. ¹H and ¹³C NMR spectra were measured on a Bruker ARX 400 spectrometer using chloroform-*d* as solvent and tetramethylsilane (TMS; $\delta = 0$ ppm) as internal standard. Agilent 5975 apparatus (EI, 70 eV) was used to obtain mass spectra. Thermogravimetric analysis (TGA) was carried on a TA TGA Netzsch TG209 under dry nitrogen at a heating rate of 10 °C min⁻¹. UV-vis absorption spectra were measured on a Varian CARY 100 Bio spectrophotometer. Photoluminescence (PL) spectra were recorded on a Perkin-Elmer LS 55 spectrofluorometer. Weight (M_w) and number-average (M_n) molecular weights and polydispersity indices (M_w/M_n) of the polymers were estimated by a Waters Associate's gel permeation chromatography (GPC) system equipped with refractive index and UV detectors. A set of monodisperse polystyrene standards covering molecular weight range of 10³–10⁷ was used for the molecular weight calibration. THF was used as eluent at a flow rate of 1.0 mL min⁻¹.

Monomer Syntheses

Silole diyne **5**^{10(g)} was synthesized according to our published method, whereas compounds **1–4** were prepared according to the synthetic routes shown in Scheme 2. Typical experimental procedures for their syntheses are shown below.

Synthesis of 1,4-Bis(dimethylsilyl)benzene (**1**)

To a solution of 1,4-dibromobenzene (0.47 g, 2 mmol) in ether (50 mL) at -78 °C, tetramethyl ethylenediamine (TMEDA; 1.2 mL, 8 mmol) and *n*-butyllithium (1.6 M solution in hexane, 5 mL, 9 mmol) were added dropwise. The mixture was stirred at -78 °C for 1 h, and warmed to room temperature. After stirring for 1 h, the mixture was cooled to -78 °C again, to which chlorodimethylsilane (0.8 mL, 8 mmol) was added dropwise. After stirring for 30 min at -78 °C, the mixture was allowed to warm to room temperature and kept stirring overnight. The mixture was then poured into water and extracted with dichloromethane (DCM) by three times. The combined organic layers were dried over magnesium sulfate. After filtration, the solvent was evaporated by rotary evaporator. The residue was purified by column chromatography (silica gel, hexane) to give 1,4-bis(dimethylsilyl)benzene (**1**) (0.23 g, 56% yield) as colorless liquid.

IR (film), ν (cm⁻¹): 2120 (Si–H stretching), 1250 (Si–CH₃ bending), 1136 (Si–Ph stretching). ¹H NMR (400 MHz, CDCl₃), δ (TMS, ppm): 7.57 (s, 4H), 4.43–4.47 (m, 2H), 0.37 (d, 12H, $J = 3.6$ Hz). ¹³C NMR (100 MHz, CDCl₃), δ (TMS, ppm): 138.6, 133.6, -3.7 . MS (EI): 193 ($M^+ - 1$).

Other aromatic silylhydrides were prepared by a similar procedure and their characterization data are given below.

4,4'-Bis(dimethylsilyl)biphenyl (2)

Colorless liquid, yield 48%. IR (film), ν (cm^{-1}): 2118 (Si—H stretching), 1250 (Si—CH₃ bending), 1117 (Si—Ph stretching). ¹H NMR (400 MHz, CDCl₃), δ (TMS, ppm): 7.67–7.62 (m, 8H), 4.52–4.48 (m, 2H), 0.41 (d, 12H, $J = 3.6$ Hz). ¹³C NMR (100 MHz, CDCl₃), δ (TMS, ppm): 142.0, 136.5, 134.8, 126.8, –3.5. MS (EI): 270 (M^+).

2,5-Bis(dimethylsilyl)thiophene (3)

Colorless liquid, yield 51%. IR (film), ν (cm^{-1}): 2127 (Si—H stretching), 1250 (Si—CH₃ bending), 1013 (Si—Ph stretching). ¹H NMR (400 MHz, CDCl₃), δ (TMS, ppm): 7.40 (s, 2H), 4.63–4.59 (m, 2H), 0.42 (d, 12H, $J = 4.0$ Hz). ¹³C NMR (100 MHz, CDCl₃), δ (TMS, ppm): 135.8, 125.8, –2.6. MS (EI): 200 (M^+).

2,7-Bis(dimethylsilyl)-9,9-dihexylfluorene (4)

Colorless liquid, yield 56%. IR (film), ν (cm^{-1}): 2118 (Si—H stretching), 1248 (Si—CH₃ bending), 1092 (Si—Ph stretching). ¹H NMR (400 MHz, CDCl₃), δ (TMS, ppm): 7.71 (d, 2H, $J = 7.6$ Hz), 7.51 (d, 4H, $J = 6.4$ Hz), 4.53–4.49 (m, 2H), 1.99–1.95 (m, 4H), 1.07–0.65 (m, 30H), 0.45 (d, 12H, $J = 3.6$ Hz). ¹³C NMR (100 MHz, CDCl₃), δ (TMS, ppm): 150.2, 142.1, 136.2, 132.5, 128.4, 119.3, 55.0, 40.1, 31.8, 29.9, 29.2, 29.1, 23.7, 22.7, 14.1, –3.4. MS (EI): 506 (M^+).

Polymerization

All the polymerization reactions and manipulations were carried out under nitrogen, except for the purification of the polymers, which was done in open air. A typical experimental procedure for the polymerization of silole diyne **5** with **1** is given below as an example. Into a baked 25-mL flask, silole diyne **5** (46.3 mg, 0.1 mmol), 1,4-bis(dimethylsilyl)benzene (**1**) (20 mg, 0.1 mmol), and Rh(PPh₃)₃Cl (1.3 mg, 0.0014 mmol) were added. The flask was evacuated under vacuum for half an hour and then flushed with nitrogen. Freshly distilled THF (2 mL) was injected into the flask to dissolve the monomers. After refluxing for 12 h under nitrogen, the solution was then cooled to room temperature and was added into ethanol (150 mL) through a cotton filter under stirring. The precipitates were collected and dissolved in THF (3 mL) and were precipitated from ethanol for two more times. After filtration, the polymer was dried in vacuum oven at 40 °C to a constant weight. The polymer **P1/5** was obtained as yellowish powder in 92% yield. M_w 95,300; M_w/M_n 2.8 (GPC, polystyrene calibration).

IR (KBr), ν (cm^{-1}): 1248 (Si—CH₃ bending), 1133 (Si—Ph stretching). ¹H NMR (400 MHz, CDCl₃), δ (TMS, ppm): 7.52 (Ar-H), 7.19 (Ar-H), 7.00–6.78 (Ar-H and *E*-ArCH=), 6.47 (*E*-SiCH=), 0.46–0.38 [Si(CH₃)₂]. ¹³C NMR (100 MHz, CDCl₃), δ (TMS, ppm): 154.2, 145.1, 141.1, 139.9, 139.5, 138.8, 135.3, 133.2, 129.9, 129.1, 128.7, 127.5, 126.5, 126.3, 126.2, 126.1, –2.6, –3.6.

Other polymers were prepared by a similar procedure and their characterization data are given below.

P2/5

Yellowish powder, yield 90%. M_w 23,000; M_w/M_n 3.0 (GPC, polystyrene calibration). IR (KBr), ν (cm^{-1}): 1249 (Si—CH₃

bending), 1114 (Si—Ph stretching). ¹H NMR (400 MHz, CDCl₃), δ (TMS, ppm): 7.63–7.56 (Ar-H), 7.23–7.21 (Ar-H), 7.01–6.78 (Ar-H and *E*-ArCH=), 6.50 (*E*-SiCH=), 0.46–0.42 [Si(CH₃)₂]. ¹³C NMR (100 MHz, CDCl₃), δ (TMS, ppm): 154.2, 145.2, 141.7, 138.8, 135.3, 134.4, 130.0, 129.2, 128.8, 127.5, 126.6, 126.3, 126.0, –2.4, –3.7.

P3/5

Yellowish powder, yield 85%. M_w 30,800; M_w/M_n 2.8 (GPC, polystyrene calibration). IR (KBr), ν (cm^{-1}): 1249 (Si—CH₃ bending), 1008 (Si—Ar stretching). ¹H NMR (400 MHz, CDCl₃), δ (TMS, ppm): 7.34 (Ar-H), 7.22–7.20 (Ar-H), 7.00–6.76 (Ar-H and *E*-ArCH=), 6.47 (*E*-SiCH=), 0.46–0.44 [Si(CH₃)₂]. ¹³C NMR (100 MHz, CDCl₃), δ (TMS, ppm): 154.2, 145.2, 144.4, 141.5, 140.0, 138.8, 135.9, 135.2, 128.7, 128.4, 128.0, 127.5, 126.6, 125.7, –1.2, –3.6.

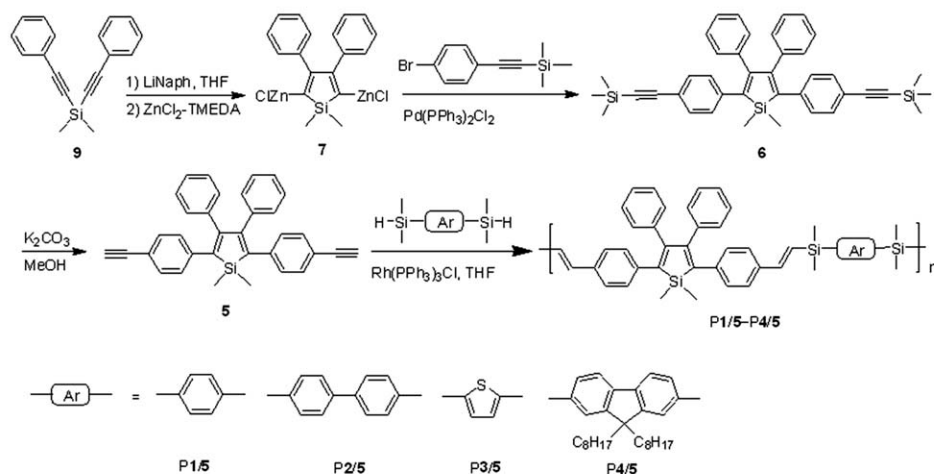
P4/5

Yellowish powder, yield 82%. M_w 14,900; M_w/M_n 1.8 (GPC, polystyrene calibration). IR (KBr), ν (cm^{-1}): 1247 (Si—CH₃ bending), 1091 (Si—Ar stretching). ¹H NMR (400 MHz, CDCl₃), δ (TMS, ppm): 7.67 (Ar-H), 7.48 (Ar-H), 7.21–7.19 (Ar-H), 7.00–6.78 (Ar-H and *E*-ArCH=), 6.53 (*E*-SiCH=), 1.93 [C(CH₂)₂], 1.25–0.62 [(CH₂)₆CH₃], 0.45–0.42 [Si(CH₃)₂]. ¹³C NMR (100 MHz, CDCl₃), δ (TMS, ppm): 154.2, 150.2, 145.0, 141.9, 141.5, 139.9, 138.8, 137.1, 135.4, 132.5, 129.9, 129.1, 128.6, 128.2, 127.5, 126.7, 126.5, 126.3, 126.2, 119.2, 54.9, 40.0, 31.8, 29.9, 29.2, 29.1, 23.8, 22.6, 14.1, –2.2, –3.7.

RESULTS AND DISCUSSION

Monomer Syntheses

Since the first observation of novel AIE phenomenon from 1-methyl-1,2,3,4,5-pentaphenylsilole,^{2(a)} we have been working on design and syntheses of new silole molecules with specific chemical structures and functionalities. The endeavors have enabled us to get various silole derivatives with potential applications in materials science and biological process, and have better understanding on the structure–property relationships of silole-based materials. 2,5-Bis(4-ethynylphenyl)-1,1-dimethyl-3,4-diphenylsilole (**5**) is an interesting silole derivative bearing two acetylene groups at the periphery, which has been used to build hyperbranched polymer through cyclotrimerization polymerization.^{10(g)} In this work, we use silole derivative as one of the monomers for the hydrosilylation polymerization. Scheme 1 illustrates the synthetic route to **5**, and the detailed procedures had been presented in our previous publication.^{10(g)} On the other hand, we designed a group of aromatic silylhydrides (**1–4**), whose synthetic routes are shown in Scheme 2. These aromatic silylhydrides were successfully prepared in moderate yields of (48–56%) by lithiation of aryl bromide with *n*-butyllithium in the presence of TMEDA, and followed treatment with chlorodimethylsilane. The addition of TMEDA was helpful to stabilize the lithiated intermediates, and thus increase reactions yields. All the structures of the monomers were confirmed by standard spectroscopic methods with satisfactory data.



SCHEME 1 Syntheses of silole diyne **5** and its hydrosilylation polymerization with aromatic silylhydrides.

Polymerization

Hydrosilylations of alkynes are commonly catalyzed by transition metal catalysts, such as $\text{Rh}(\text{PPh}_3)_3\text{Cl}$, H_2PtCl_6 , Karstedt's catalyst, and so forth. Our previous works showed that the alkyne polyhydrosilylations underwent regioselectively in the presence of rhodium catalyst $[\text{Rh}(\text{PPh}_3)_3\text{Cl}]$ in moderate yields (55.9–78.1%).¹⁷ Herein, the $\text{Rh}(\text{PPh}_3)_3\text{Cl}$ was also used to catalyze polymerization reactions of these new monomers. To further increase reaction yields and get high molecular weights, the polymerization conditions including solvents, concentration, time, and the amounts of the catalyst were investigated using the polymerization of **1** and **5** as an example. As can be seen in Table 1, reaction yields and molecular weights became higher by prolonging reaction time gradually from 4 to 12 h. Lowering the fraction (mol %) of catalyst from 1.4 to 0.5% relative to monomer decreased reaction yields slightly but caused notable detrimental effect to the molecular weight. The effects of the monomers concentrations were also tested. Reaction with a moderate monomer concentration of 0.1 mM showed higher yields and higher molecular weights than those with doubled or halved concentrations. Moreover, the reaction carried out in THF offered better results than in toluene, suggesting that the polar solvents were more suitable for the hydrosilylation

polymerization. Under optimum conditions, polymers **P1/5**–**P4/5** with high molecule weights (14,900–95,300) were synthesized in high yields in (82–92%). All the polymers are readily soluble in common organic solvents, such as THF, toluene, DCM, and chloroform, which are partially attributed to the flexible sp^3 hybridized silicon bridges.

Structural Characterization

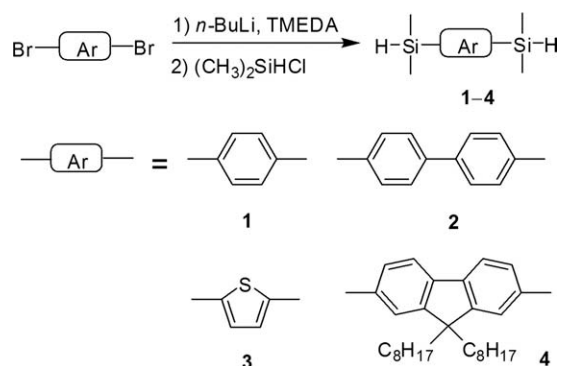
The structures of new polymeric products were characterized by IR and NMR spectroscopies and satisfactory analysis data corresponding to their expected molecular structures were obtained. An IR spectrum of **P1/5** is shown in Figure 1

TABLE 1 Syntheses of Silole-Containing Poly(silylenevinylene)s^a

No.	Polymer	Solvent ([1–5], M)	Catalyst (mM)	Time (h)	M_w^b	M_n^b	Yield (%)
1	P1/5	THF (0.05)	0.7	4	27,800	4.0	82
2	P1/5	THF (0.05)	0.7	8	48,400	4.5	89
3	P1/5	THF (0.05)	0.7	12	95,300	2.8	92
4	P1/5	THF (0.05)	0.55	12	74,800	4.0	91
5	P1/5	THF (0.05)	0.25	12	34,500	2.9	88
6	P1/5	THF (0.1)	1.1	12	36,800	4.6	89
7	P1/5	THF (0.025)	0.275	12	13,500	2.4	75
8	P1/5	Toluene (0.05)	0.55	12	23,500	3.4	87
9	P2/5	THF (0.05)	0.55	12	14,300	2.3	83
10	P2/5	THF (0.05)	0.7	12	23,000	3.0	90
11	P3/5	THF (0.05)	0.55	12	25,300	3.3	82
12	P3/5	THF (0.05)	0.7	12	30,800	2.8	85
13	P4/5	THF (0.05)	0.55	12	12,600	2.1	84
14	P4/5	THF (0.05)	0.7	12	14,900	1.8	82

^a Carried out in refluxed THF under nitrogen using $\text{Rh}(\text{PPh}_3)_3\text{Cl}$ as catalyst. For the reaction using toluene as solvent, temperature was kept at 70 °C. Concentration: [1–4] = [5].

^b Determined by GPC in THF on the basis of a polystyrene calibration.



SCHEME 2 Syntheses of aromatic silylhydrides.

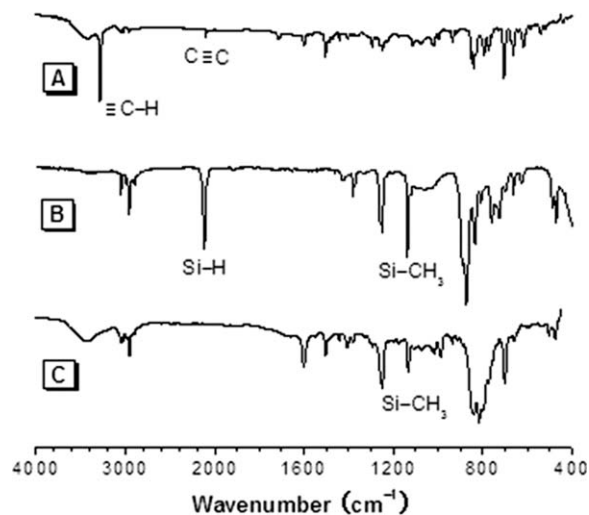


FIGURE 1 IR spectra of (A) **5**, (B) **1**, and (C) P1/5.

as an example. The spectra of monomers **1** and **5** are also given in the same figure for the sake of comparison. The $\equiv\text{C-H}$ and $\text{C}\equiv\text{C}$ stretching vibrations of **5** occur at 3286 and 2104 cm^{-1} , respectively, which are not observed in P1/5. The IR spectrum of **1** shows Si-H stretching vibration at 2120 cm^{-1} , which is absent in P1/5. While the Si-CH₃ bending vibration at 1250 cm^{-1} derived from monomer **1** is discernible in the IR spectrum of P1/5. Moreover, the peak around 1600 cm^{-1} associated with C=C stretching vibration

becomes broader and stronger after the polymerization, revealing that the triple bonds in **5** and the dimethylsilyl groups in **1** have been transformed into vinyl silylene units in P1/5. Similar features are also observed from the IR spectra of P2/5–P4/5.

The NMR analyses are also carried out to confirm the polymer structures, the results from which agree with above observations. Figure 2 shows the ¹H NMR spectra of P1/5 and monomers **1** and **5** in chloroform-*d*. The acetylene and Si-H proton resonances of **5** and **1** at δ 3.05 and 4.45, respectively, are disappeared in the NMR spectrum of P1/5. Meanwhile, new peaks at δ 6.47 and 6.81 are found, which are assigned to the proton absorptions of the linear *E*-vinylene structure,¹⁷ but the associated absorptions of the *Z*-vinylene protons around δ 6.00 are hardly discernible, suggesting that the hydrosilylation catalyzed by Rh(PPh₃)₃Cl is regioselective, which is in accordance with our previous findings.¹⁷ No unexpected peaks are found, and all the peaks can be readily assigned. Thus, the polymeric product is indeed P1/5 with a regular molecular structure as shown in Scheme 1. Similar observations were found in the spectra of P2/5–P4/5 with dominative *E* contents. The structures of the polymer were further investigated by ¹³C NMR analysis. The ¹³C NMR spectra of P1/5, **1**, and **5** are shown in Figure 3. The acetylene carbon atoms of **5** resonate at δ 84.0 and 77.3 but similar peaks are absent in the spectra of P1/5–P4/5, indicating that most acetylene units have reacted with dimethylsilyl groups.

Thermal Stability

The thermal stabilities of these silole-containing polymers were evaluated by TGA. As shown in Figure 4, all the

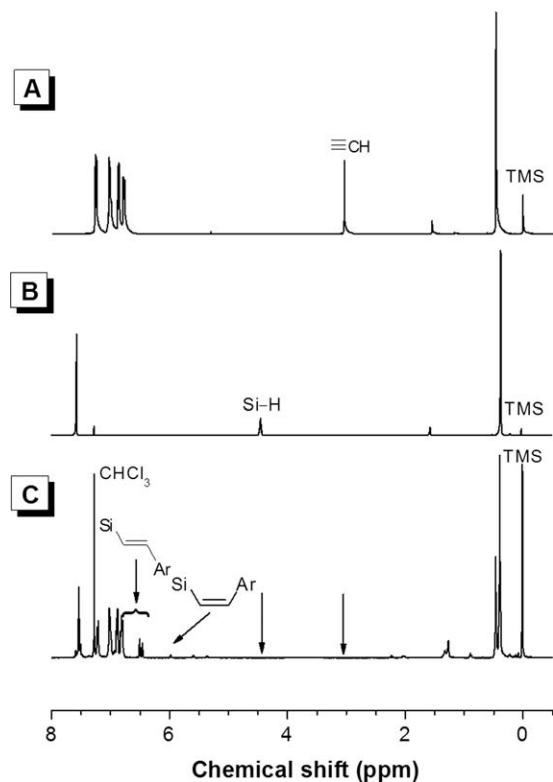


FIGURE 2 ¹H NMR spectra of (A) **5**, (B) **1**, and (C) P1/5 in chloroform-*d*.

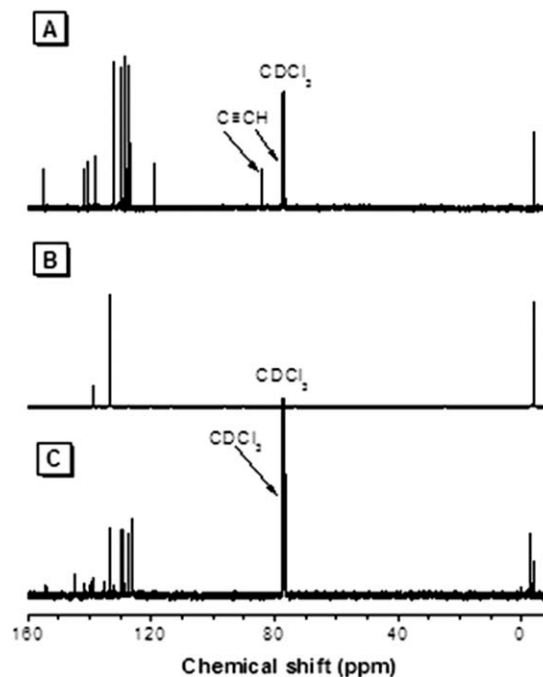


FIGURE 3 ¹³C NMR spectra of (A) **5**, (B) **1**, and (C) P1/5 in chloroform-*d*.

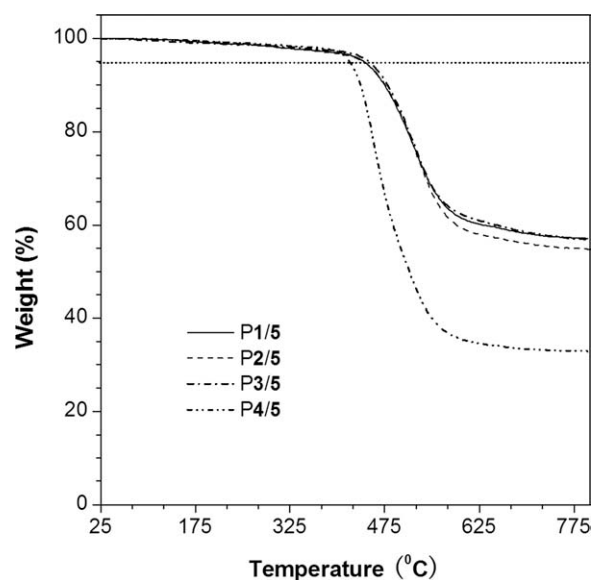


FIGURE 4 TGA thermograms of P1/5–P4/5 recorded under nitrogen at a heating rate of $10\text{ }^{\circ}\text{C min}^{-1}$.

polymers are thermally stable. The P1/5–P3/5 lose 5% of their weights (T_d) at 441–449 $^{\circ}\text{C}$ (Table 1), which are higher than that of P4/5 (420 $^{\circ}\text{C}$). The higher T_d s of P1/5–P3/5 are understandable because they are constructed mainly from aromatic rings without long alkyl chains, which possess a high resistance to thermolysis. Moreover, P1/5–P3/5 remain about 60% weight even at temperatures up to 750 $^{\circ}\text{C}$, which is attributable to their high silicon contents and/or possible crosslinking reaction. Such good thermal properties reveal their potential utility as ceramic precursors.

Optical Property

Figure 5 shows the absorption spectra of the silole-containing poly(silylenevinylene)s in their dilute THF solutions. P1/

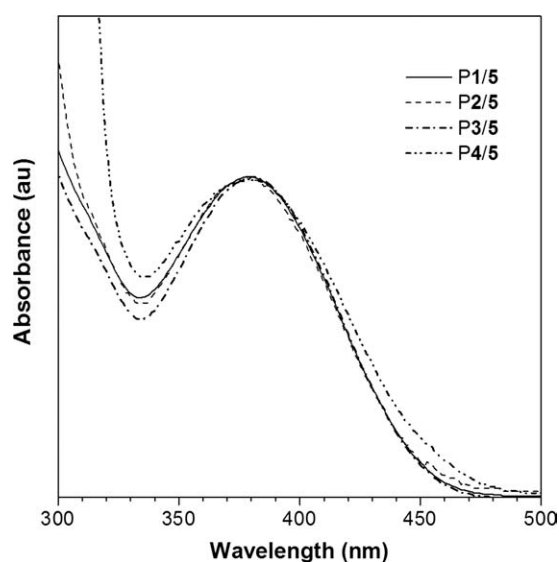


FIGURE 5 Absorption spectra of P1/5–P4/5 in dilute THF solutions (10 μM).

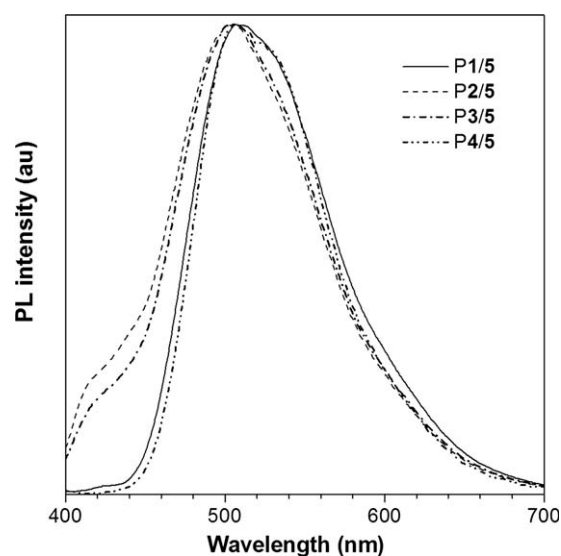


FIGURE 6 PL spectra of P1/5–P4/5 in dilute THF solutions (10 μM).

5–P4/5 show similar absorption spectra with absorption maxima in the range of 380–384 nm. Similarly, P1/5–P4/5 show close PL at $\sim 506\text{ nm}$ (Fig. 6). However, the emissions of P1/5–P4/5 are quite weak when molecularly dissolved in dilute THF solutions (10 μM). Their fluorescence quantum yields (Φ_F) measured using 9,10-diphenylanthracene as standard are rather low (0.99–1.44%, Table 2), which are much lower than those of biphenyl, fluorene,¹⁸ and their polymeric derivatives. Similar phenomena are also observed when covalently connecting conventional chromophores (pyrene, anthracene, fluorene, carbazole, etc.) with AIE luminogens (TPE and silole) in our previous works.¹⁹ The intramolecular rotations (IMR) of the phenyl blades attached at the silole stator have effectively consumed the excited state energy of the polymers, rendering quite weak emission in the solution state. These polymers become emissive when fabricated as thin solid films. The films of P1/5–P4/5 show

TABLE 2 Optical and Thermal Properties and Quenching Constants of Silole-Containing Poly(silylenevinylene)s^a

	λ_{abs} (nm)	λ_{em} (nm)		Φ_F (%)		T_d ($^{\circ}\text{C}$)	K (L mol^{-1})
		Soln	Aggr	Soln ^b	Film ^c		
P1/5	383	507	512	0.99	7.7	442	6,220
P2/5	384	506	512	1.19	22.0	441	27,368
P3/5	380	505	511	1.44	10.6	449	20,107
P4/5	381	507	506	1.25	11.6	420	27,949

^a Abbreviation: soln, dilute THF solution; aggr, aggregates in aqueous mixture; film, drop-casted film on quartz; T_d , decomposition temperature for 5% weight loss; λ_{abs} , absorption maximum in THF solution; λ_{em} , emission maximum.

^b Fluorescence quantum yield in THF solution measured using 9,10-diphenylanthracene as standard ($\Phi_F = 90\%$ in cyclohexane).

^c Fluorescence quantum yield of the solid film measured by an calibrated integrating sphere.

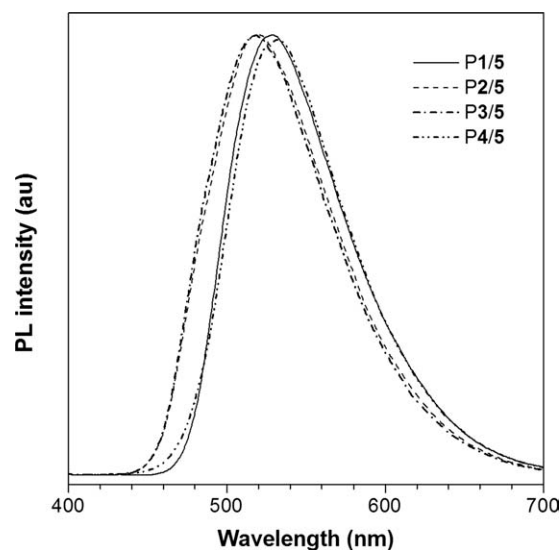


FIGURE 7 PL spectra of P1/5–P4/5 in film state.

green emission peaked at 519–533 nm (Fig. 7), which are bathochromically shifted compared with those in solutions. This can be interpreted as caused by active intermolecular interactions between aromatic rings in the condensed phase. Much higher Φ_F values (7.7–22.0%) than those in solutions are measured from the polymers films by a calibrated integrating sphere, which are comparable with those of reported silole- or TPE-based polymers.^{10(g),17} The greatly enhanced emission efficiencies of the polymers in the solid state suggest that they are of aggregation-enhanced emission (AEE) characteristics.

To further confirm the AEE characteristics of these silole-containing poly(silylenevinylene)s, we measured their PL spectra in THF/water mixtures with different water fractions (f_w vol %). Figure 8(A) displays the PL spectra of polymer

P4/5 in THF/water mixture as an example. As indicated in the figure, the emission intensity enhanced gradually with the increase of f_w . This is because that addition of a large amount of water into the THF solution of polymer P4/5 causes its molecules to aggregate, due to the immiscibility of the hydrophobic polymer with the hydrophilic medium. The aggregate formation restricts the IMR, and thus blocks the channel of nonradiative decay, changing the polymer to a strong emitter. Clearly, polymer P4/5 is AEE active. It is AEE active because the emission of the polymer in the solution state is not completely quenched by IMR process of phenyl blades of siloles.^{2,3} In the polymer systems, the silole units are covalently embedded in the conjugated polymer backbone, and meantime, polymer chains may adopt entangled conformations, both of which have inhibited the IMR process in some extent and thus reduced nonradiative energy decay. This is different from its AIE-active silole monomer, whose light emission in solution is severely extinguished by IMR process. The AEE effect is not an isolated case observed in P4/5, and P1/5–P3/5 exhibit similar emission enhancement behaviors (Supporting Information Figs. S1–S3).

Explosive Detection

Rapid detection of explosives is greatly demanded in an effort to better combat terrorism and control environmental pollution. The success in the detection of explosives using AIE- or AEE-active small molecules and polymers encourages us to explore the utility as chemosensors of these new silole-containing poly(silylenevinylene)s. With this in mind, we monitor the PL changes of polymers in both solution and aggregate states in the presence of PA. PA is used as a model compound for it is commercially available and widely used in the manufacture of rocket fuels, fireworks, matches, and so forth,²⁰ whose explosive power is somewhat superior to that of TNT. Figure 9(A,B) shows the PL spectra of polymer P4/5 in THF solutions and in THF/water mixtures ($f_w = 90\%$) on PA addition, respectively. In THF solution, the PA

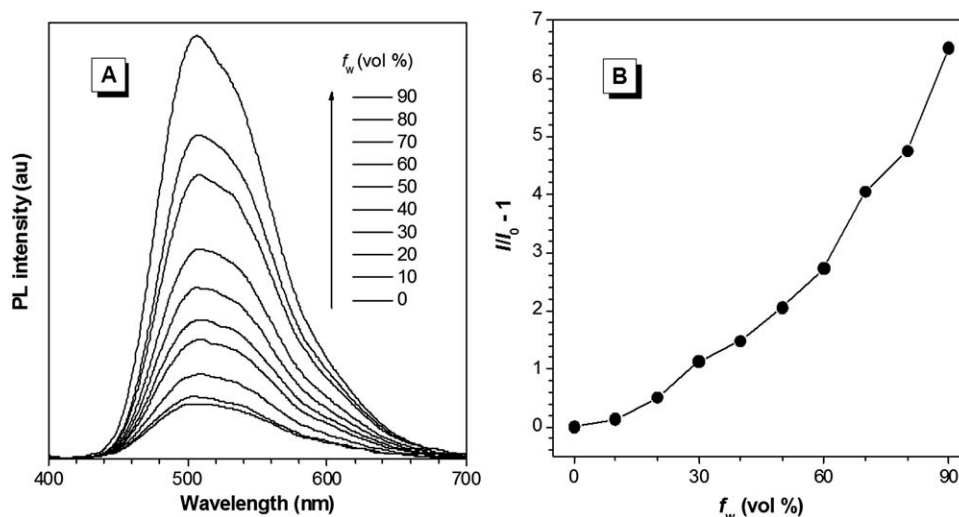


FIGURE 8 (A) PL spectra of P4/5 in THF and THF/water mixtures with different water fractions. (B) Changes in the relative PL intensity (I/I_0) with the composition of the THF/water mixture. I_0 = PL intensity in pure THF solution. Concentration: 10^{-5} M; excitation wavelength: 350 nm.

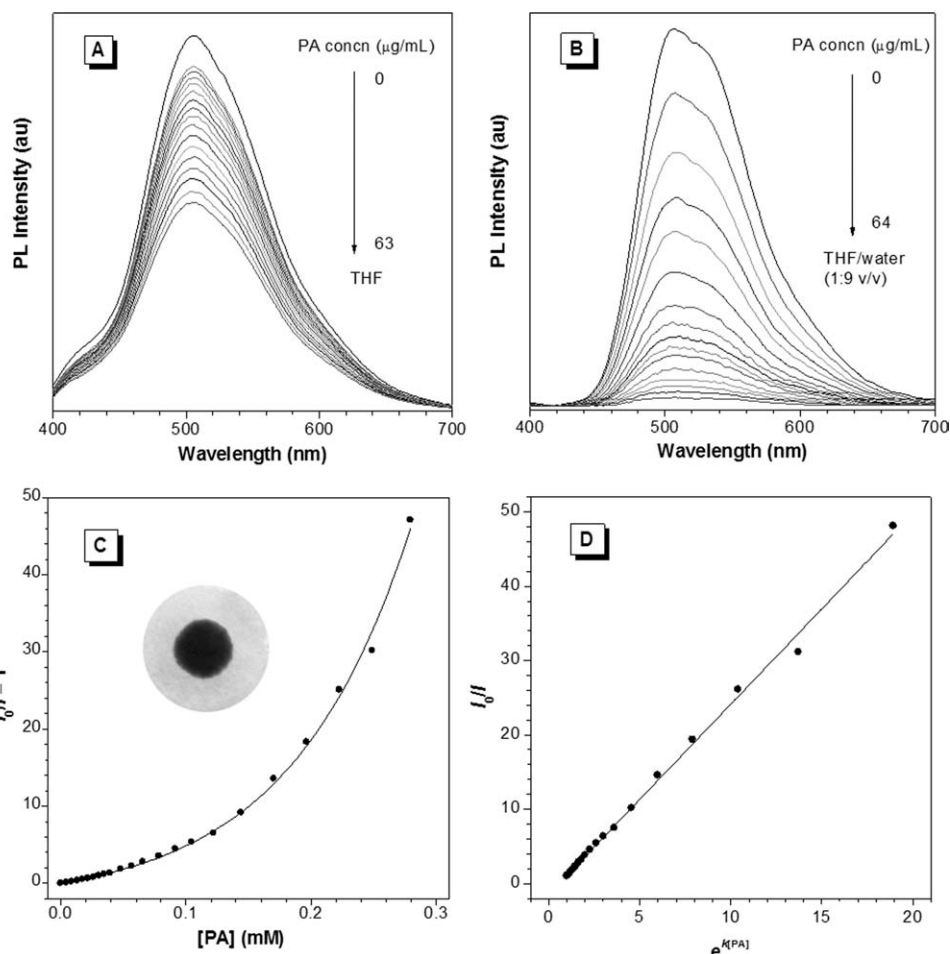


FIGURE 9 Fluorescence quenching of P4/5 in (A) THF and (B) THF/water mixture (1:9 v/v) by PA. Concentration of P4/5: 10^{-5} M; excitation wavelength: 350 nm. (C) Stern–Volmer plot of $I_0/I - 1$ value versus [PA] in THF/water mixture (1:9 v/v). I_0 = PL intensity in the absence of PA. (D) Plot of I_0/I value versus $e^{k[PA]}$ in THF/water mixture (1:9 v/v). Inset in panel C: fluorescence image of P4/5 deposited on a filter paper with a spot of PA solution under UV illumination.

addition causes decrease in PL intensity of P4/5 in some extent but the light emission is not totally quenched even a large amount of PA is added. The inferior quenching effect is partially due to its weak emission in the dispersive state. The aggregates of P4/5 in THF/waters mixture ($f_w = 90\%$), however, show sensitive response to PA. The emission is progressively weakened with increase of PA concentration ([PA]). The detection is of high sensitivity, and emission quenching can be clearly discerned at a [PA] as low as 1 ppm. At a [PA] of $64 \mu\text{g mL}^{-1}$, virtually no light is observed from the 90% aqueous mixture. The Stern–Volmer plot of relative PL intensity ($I_0/I - 1$) versus [PA] gives a curve bending upward [Fig. 9(C)], instead of a linear line, revealing a superamplification effect in the emission quenching process. According to our previous findings,^{10(g),11} it is considered that the fluorescence annihilation of polymer aggregates should be in a static quenching fashion that gives nonlinear Stern–Volmer plots. The effective quenching sphere model (eq 1) can be used to describe the quenching process by the static mechanism.

$$\frac{I_0}{I} = Ae^{k[PA]} + B \quad (1)$$

where A and B are constants, and k denotes the static quenching constant. By fitting the Stern–Volmer plot shown in Figure 9(C), eq 2 is obtained

$$\frac{I_0}{I} = 2.60e^{10.526[PA]} - 1.55 \quad (2)$$

When the [PA] is very low, eq (1) can be transformed to eq (3) using a mathematical treatment of Taylor expansion:

$$\frac{I_0}{I} = A(1 + k[PA]) + B = Ak[PA] + A + B = K[PA] + C \quad (3)$$

where $K = kA$ and $C = A + B = 1$. Therefore, the static quenching constant or the K value of the Stern–Volmer plot for polymer P4/5 aggregates in THF/water mixture ($f_w = 90\%$) is $27,368 \text{ L mol}^{-1}$. By plotting the relative PL intensity (I_0/I) versus $e^{k[PA]}$, a linear line is obtained [Fig. 9(D)] with a

k value of 10,526, which enables quantitative analysis. The quenching constant K value is higher than those of the reported poly(tetraphenylsilole-vinylene) and other linear polysiloles ($<20,000 \text{ L mol}^{-1}$).^{14(a),14(e)} Similar sensing capabilities are also observed from P1/5, P2/5, and P3/5, with K values of 6220, 20,107, and 27,949 L mol^{-1} , respectively (Supporting Information Figs. S4–S6). The K values of P2/5–P4/5 are higher than that of P1/5, which is probably due to the higher emission efficiencies in the aggregate state and better electron-donating abilities of aromatic segments in P2/5–P4/5 that promote the potentially involved Lewis acid–base interactions between the polymers and the PA analytes.^{10(g),14(e)}

Generally, the aggregate formation of polymers composed by the conventional ACQ chromophores weakens the light emission due to the formation of detrimental species, such as excimers and exciplexes. Such ACQ effect is disadvantageous to sensing performances of the polymers. While polymers created using AIE units exhibit opposite emission behaviors. These silole-containing polymers are emissive in aggregate state, which is beneficial to the sensitivity of detection. Moreover, the aggregates possess numerous cavities for the quencher molecules to entry in, offering additional inter-branched diffusion channels for exciton migration.¹¹ Therefore, the superquenching effect can be interpreted as a cooperative effect of the emission quenching by the PA molecules binding in the inner cavities and outer surfaces through electron donor–acceptor interaction and/or energy transfer.

Since these polymers are emissive in the film state, the explosive detection that can be carried out using polymer-coated strips is predictable. A prototype of a solid-state chemosensor is prepared by simply dipping a filter paper into a polymer P4/5 solution. The emissive test paper is obtained after solvent evaporation. The detection process is fast and the assay procedure is simple. When a PA solution is dropped onto the test paper, the PA-covered spot become nonfluorescent, which is vividly discernable to the naked eye as seen from the example shown in the inset of Figure 9(C), under UV illumination. The results suggest that these silole-containing poly(silylenevinylene)s are promising candidates for portable sensitive chemosensor devices for explosive detection.

CONCLUSIONS

In summary, a series of silole-containing poly(silylenevinylene)s with high molecular weights are regioselectively synthesized in high yields by Rh(PPh₃)₃Cl-catalyzed hydrosilylation polymerization of 2,5-bis(4-ethynylphenyl)silole with aromatic silylhydrides in refluxed THF. All the polymers are soluble and processable. They enjoy high thermal stability with decomposition temperatures in the range of 420–449 °C. The polymers are weakly fluorescent in the solution state but become strong emitters when aggregated in poor solvents or fabricated as thin films, exhibiting a feature of AEE. The emissions of the polymers aggregates are quenched exponentially by PA with high quenching constants up to

27,949 L mol^{-1} , demonstrating a superamplification effect. These results suggest that they are promising candidates for sensitive explosive detection.

The authors acknowledge financial support from National Natural Science Foundation of China (21074028 and 21104012), Natural Science Foundation of Zhejiang Province (Y4110331), and the Research Grant Council of Hong Kong (HKUST2/CRF/10 and N_HKUST620/11).

REFERENCES AND NOTES

- (a) Khabashesku, V. N.; Balaji, V.; Boganov, S. E.; Nefedov, O. M.; Michl, J. *J. Am. Chem. Soc.* **1994**, *116*, 320–329; (b) Tamao, K.; Yamaguchi, S.; Ito, Y.; Matsuzaki, Y.; Yamabe, T.; Fukushima, M.; *Macromolecules* **1995**, *28*, 8668–8675; (c) Tamao, K.; Ohno, S.; Yamaguchi, S. *Chem. Commun.* **1996**, 1873–1874; (d) Yamaguchi, S.; Tamao, K. *J. Chem. Soc., Dalton Trans.* **1998**, 3693–3702; (e) Chan, L. H.; Lee, R. H.; Hsieh, C. F.; Yeh, H. C.; Chen, C. T. *J. Am. Soc. Chem.* **2002**, *124*, 6469–6479; (f) Chan, L. H.; Yeh, H. C.; Chen, C. T. *Adv. Mater.* **2001**, *13*, 1637–1641; (g) Murata, H.; Malliaras, G. G.; Uchida, M.; Shen, Y.; Kafafi, Z. H. *Chem. Phys. Lett.* **2001**, *339*, 161–166; (h) Mäkinen, A. J.; Uchida, M.; Kafafi, Z. H. *J. Appl. Phys.* **2004**, *95*, 2832–2838.
- (a) Luo, J.; Xie, Z.; Lam, J. W. Y.; Cheng, L.; Chen, H.; Qiu, C.; Kwok, H. S.; Zhan, X.; Liu, Y.; Zhu, D.; Tang, B. Z. *Chem. Commun.* **2001**, 1740–1741; (b) Hong, Y.; Lam, J. W. Y.; Tang, B. Z. *Chem. Commun.* **2009**, 4332–4353; (c) Liu, J.; Lam, J. W. Y.; Tang, B. Z. *J. Inorg. Organomet. Polym. Mater.* **2009**, *19*, 249–285; (d) Hong, Y.; Lam, J. W. Y.; Tang, B. Z. *Chem. Soc. Rev.* **2011**, *40*, 5361–5388; (e) Qin, A.; Lam, J. W. Y.; Tang, B. Z. *Prog. Polym. Sci.* **2012**, *37*, 182–209.
- (a) Li, Z.; Dong, Y.; Mi, B.; Tang, Y.; Häußler, M.; Tong, H.; Dong, Y.; Lam, J. W. Y.; Ren, Y.; Sun, H. H. Y.; Wong, K. S.; Gao, P.; Williams, I. D.; Kwok, H. S.; Tang, B. Z. *J. Phys. Chem. B* **2005**, *109*, 10061–10066; (b) Dong, Y.; Lam, J. W. Y.; Li, Z.; Tong, H.; Dong, Y.; Feng, X. D.; Tang, B. Z. *J. Inorg. Organomet. Polym. Mater.* **2005**, *15*, 287–291; (c) Zhao, Z.; Wang, Z.; Lu, P.; Chan, C. Y. K.; Liu, D.; Lam, J. W. Y.; Sung, H. H. Y.; Williams, I. D.; Ma, Y.; Tang, B. Z. *Angew. Chem. Int. Ed.* **2009**, *48*, 7608–7611; (d) Yu, G.; Yin, S.; Liu, Y.; Chen, J.; Xu, X.; Sun, X.; Ma, D.; Zhan, X.; Peng, Q.; Shuai, Z.; Tang, B. Z.; Zhu, D.; Fang, W.; Luo, Y. *J. Am. Chem. Soc.* **2005**, *127*, 6335–6346.
- (a) Tamao, K.; Uchida, M.; Izumizawa, T.; Fukukawa, K.; Yamaguchi, S. *J. Am. Chem. Soc.* **1996**, *118*, 11974–11975; (b) Uchida, M.; Izumizawa, T.; Nakano, T.; Yamaguchi, S.; Tamao, K.; Furukawa, K. *Chem. Mater.* **2001**, *13*, 2680–2683; (c) Murata, H.; Kafafi, Z. H.; Uchida, M. *Appl. Phys. Lett.* **2002**, *80*, 189–191; (d) Liu, Y.; Chen, Z.; Chen, J.; Wang, F.; Cao, Y. *Polym. Bull.* **2007**, *59*, 31–44; (e) Geramita, K.; McBee, J.; Shen, Y.; Radu, N.; Tilley, T. D. *Chem. Mater.* **2006**, *18*, 3261–3265; (f) Son, H.-J.; Han, W.-S.; Chun, J.-Y.; Lee, C.-J.; Han, J.-I.; Ko, J.; Kang, S. O. *Organometallics* **2007**, *26*, 519–526; (g) Tang, B. Z.; Zhan, X.; Yu, G.; Lee, P. P. S.; Liu, Y.; Zhu, D. *J. Mater. Chem.* **2001**, *11*, 2974–2978; (h) Zhao, Z.; Chen, S.; Lam, J. W. Y.; Jim, C. K. W.; Chan, C. Y. K.; Wang, Z.; Lu, P.; Kwok, H. S.; Ma, Y.; Tang, B. Z. *J. Phys. Chem. C* **2010**, *114*, 7963–7972; (i) Du, X.; Wang, Z. Y. *Chem. Commun.* **2011**, 47, 4276–4278.
- (a) Mi, B.; Dong, Y.; Li, Z.; Lam, J. W. Y.; Häußler, M.; Sung, H. H. Y.; Kwok, H. S.; Dong, Y.; Williams, I. D.; Liu, Y.; Luo, Y.; Shuai, Z.; Zhu, D.; Tang, B. Z. *Chem. Commun.* **2005**, 3583–3585; (b) Wang, F.; Luo, J.; Yang, K.; Chen, J.; Huang, F.; Cao, Y. *Macromolecules* **2005**, *38*, 2253–2260; (c) Chen, J.; Cao,

- Y. *Macromol. Rapid Commun.* **2007**, *28*, 1714–1742; (d) Hong, Y.-R.; Wong, H.-K.; Moh, L. C. H.; Tan, H.-S.; Chen, Z.-K. *Chem. Commun.* **2011**, *47*, 4920–4922; (e) Song, J.; Du, C.; Li, C.; Bo, Z. *J. Polym. Sci. Part A: Polym. Chem.* **2011**, *49*, 4267–4274.
- 6** (a) Yu, Y.; Feng, C.; Hong, Y.; Liu, J.; Chen, S.; Ng, K. M.; Luo, K. Q.; Tang, B. Z. *Adv. Mater.* **2011**, *23*, 3298–3302; (b) Yu, Y.; Hong, Y.; Feng, C.; Liu, J.; Lam, J. W. Y.; Faisal, M.; Ng, K. M.; Luo, K. Q.; Tang, B. Z. *Sci. China Ser. B: Chem.* **2009**, *52*, 15–19; (c) Faisal, M.; Yu, Y.; Lam, J. W. Y.; Liu, J.; Zhang, B.; Lu, P.; Zhang, X.; Tang, B. Z. *Adv. Funct. Mater.* **2011**, *21*, 1733–1740.
- 7** (a) Li, Z.; Dong, Y.; Lam, J. W. Y.; Sun, J.; Qin, A.; Häußler, M.; Dong, Y.; Sung, H. H. Y.; Williams, I. D.; Kwok, H. S.; Tang, B. Z. *Adv. Funct. Mater.* **2009**, *19*, 905–917; (b) Hatano, K.; Saeki, H.; Yokota, H.; Aizawa, H.; Koyama, T.; Matsuoka, K.; Terunuma, D. *Tetrahedron Lett.* **2009**, *50*, 5816–5819; (c) Toal, S. J.; Jones, K. A.; Magde, D.; Trogler, W. C. *J. Am. Chem. Soc.* **2005**, *127*, 11661–11665; (d) Dong, Y.; Lam, J. W. Y.; Qin, A.; Li, Z.; Liu, J.; Sun, J. Z.; Dong, Y.; Tang, B. Z. *Chem. Phys. Lett.* **2007**, *446*, 124–127; (e) Wang, M.; Zhang, D.; Zhang, G.; Tang, Y.; Wang, S.; Zhu, D. *Anal. Chem.* **2008**, *80*, 6443–6448; (f) Liu, Z.; Xue, W.; Cai, Z.; Zhang, G.; Zhang, D. *J. Mater. Chem.* **2011**, *21*, 14487–14491; (g) Liu, Y.; Tang, Y.; Barashkov, N. N.; Irgibaeva, I. S.; Lam, J. W. Y.; Hu, R.; Birimzhanova, D.; Yu, Y.; Tang, B. Z. *J. Am. Chem. Soc.* **2010**, *132*, 13951–13953; (h) Zhao, Z.; Liu, J.; Lam, J. W. Y.; Chan, C. Y. K.; Qiu, H.; Tang, B. Z. *Dyes Pigments* **2011**, *91*, 258–263.
- 8** (a) Steinfeld, J. I.; Wormhoudt, J. *Annu. Rev. Phys. Chem.* **1998**, *49*, 203–232; (b) Albert, K. J.; Lewis, N. S.; Schauer, C. L.; Sotzing, G. A.; Stitzel, S. E.; Vaid, T. P.; Walt, D. R. *Chem. Rev.* **2000**, *100*, 2595–2626; (c) Singh, S. J. *Hazard. Mater.* **2007**, *144*, 15–28; (d) Lee, Y. H.; Liu, H.; Lee, J. Y.; Kim, S. H.; Kim, S. K.; Sessler, J. L.; Kim, Y.; Kim, J. S. *Chem. Eur. J.* **2010**, *16*, 5895–5901; (e) Xu, B.; Wu, X.; Li, H.; Tong, H.; Wang, L. *Macromolecules* **2011**, *44*, 5089–5092; (f) Cavaye, H.; Shaw, P. E.; Wang, X.; Burn, P. L.; Lo, S.-C.; Meredith, P. *Macromolecules* **2010**, *43*, 10253–10261; (g) He, G.; Yan, N.; Yang, J.; Wang, H.; Ding, L.; Yin, S.; Fang, Y. *Macromolecules*, **2011**, *44*, 4759–4766; (h) Olley, D. A.; Wren, E. J.; Vamvounis, G.; Fernee, M. J.; Wang, X.; Burn, P. L.; Meredith, P.; Shaw, P. E. *Chem. Mater.* **2011**, *23*, 789–794; (i) Tang, G.; Chen, S. S. Y.; Shaw, P. E.; Hegedus, K.; Wang, X.; Burn, P. L.; Meredith, P. *Polym. Chem.* **2011**, *2*, 2360–2368.
- 9** (a) Thomas, S. W., III; Joly, G. D.; Swager, T. M. *Chem. Rev.* **2007**, *107*, 1339–1386; (b) Zahn, S.; Swager, T. M. *Angew. Chem. Int. Ed.* **2002**, *41*, 4225–4230; (c) Bunz, U. H. F. *Chem. Rev.* **2000**, *100*, 1605–1644.
- 10** (a) Qin, A.; Lam, J. W. Y.; Tang, B. Z. *Macromolecules* **2010**, *43*, 8693–8702; (b) Qin, A.; Lam, J. W. Y.; Tang, B. Z. *Chem. Soc. Rev.* **2010**, *39*, 2522–2544; (c) Liu, J.; Lam, J. W. Y.; Tang, B. Z. *Chem. Rev.* **2009**, *109*, 5799–5867; (d) Lam, J. W. Y.; Tang, B. Z. *Acc. Chem. Res.* **2005**, *38*, 745–754; (e) Häußler, M.; Tang, B. Z. *Adv. Polym. Sci.* **2007**, *209*, 1–58; (f) Lam, J. W. Y.; Tang, B. Z. *J. Polym. Sci. Part A: Polym. Chem.* **2003**, *41*, 2607–2629; (g) Liu, J.; Zhong, Y.; Lam, J. W. Y.; Lu, P.; Hong, Y.; Yu, Y.; Yue, Y.; Faisal, M.; Sung, H. H.-Y.; Williams, I.; Wong, K. S.; Tang, B. Z. *Macromolecules* **2010**, *43*, 4921–4936;
- (h) Wang, J.; Mei, J.; Yuan, W.; Lu, P.; Qin, A.; Sun, J.; Ma, Y.; Tang, B. Z. *J. Mater. Chem.* **2011**, *21*, 4056–4059; (i) Hu, R.; Maldonado, J. L.; Rodriguez, M.; Deng, C.; Jim, C. K. W.; Lam, J. W. Y.; Yuen, M. M. F.; Ramos-Ortiz, G.; Tang, B. Z. *J. Mater. Chem.* **2012**, *22*, 232–240.
- 11** (a) Liu, J.; Zhong, Y.; Lu, P.; Hong, Y.; Lam, J. W. Y.; Faisal, M.; Yu, Y.; Wong, K. S.; Tang, B. Z. *Polym. Chem.* **2010**, *1*, 426–429; (b) Lu, P.; Lam, J. W. Y.; Liu, J.; Jim, C. K. W.; Yuan, W.; Xie, N.; Zhong, Y.; Hu, Q.; Wong, K. S.; Cheuk, K. K. L.; Tang, B. Z. *Macromol. Rapid Commun.* **2010**, *31*, 834–839.
- 12** (a) Ojima, I. In *The Chemistry Organic Silicone Compounds*; Patai, S., Rapoport, Z., Eds.; John Wiley: Chichester, UK, **1989**; p 1479; (b) Marciniak, B. *Comprehensive Handbook on Hydrosilylation*; Pergamon Press: New York, **1992**; pp 130–137; (c) Mori, A.; Takahisa, E.; Yaamamura, Y.; Kato, T.; Mudalige, A. P.; Kajiro, H.; Hirabayashi, K.; Nishihara, Y.; Hiyama, T. *Organometallics* **2004**, *23*, 1755–1765; (d) Perry, R. J.; Karageorgis, M.; Hensler, J. *Macromolecules* **2007**, *40*, 3929–3938.
- 13** (a) Ohshita, J.; Kunai, A. *Acta Polym.* **1998**, *49*, 379–403; (b) Kunai, A.; Toyoda, E.; Nagamoto, I.; Horio, T.; Ishikawa, M. *Organometallics* **1996**, *15*, 75–83; (c) Ohshita, J.; Kanaya, D.; Watanabe, T.; Ishikawa, M. *J. Organomet. Chem.* **1995**, *489*, 165–173; (d) Ohshita, J.; Matsuguchi, A.; Furumori, K.; Hong, R.-F.; Ishikawa, M. *Macromolecules* **1992**, *25*, 2134–2140; (e) Corriu, R. J. P.; Gerbler, P.; Guérin, C.; Henner, B. J. L.; Jean, A.; Mutin, P. H. *Organometallics* **1992**, *11*, 2507–2513; (f) Wu, H. J.; Interrante, L. V. *Macromolecules* **1992**, *25*, 1840–1841.
- 14** (a) Sohn, H.; Sailor, M. J.; Magde, D.; Trogler, W. C. *J. Am. Chem. Soc.* **2003**, *125*, 3821–3830; (b) Sanchez, J. C.; Trogler, W. C. *Macromol. Chem. Phys.* **2008**, *209*, 1527–1540; (c) Sanchez, J. C.; Trogler, W. C. *J. Mater. Chem.* **2008**, *18*, 3143–3156; (d) Sohn, H.; Calhoun, R. M.; Sailor, M. J.; Trogler, W. C. *Angew. Chem. Int. Ed.* **2001**, *40*, 2104–2105; (e) Sanchez, J. C.; DiPasquale, A. G.; Rheingold, A. L.; Trogler, W. C. *Chem. Mater.* **2007**, *19*, 6459–6470.
- 15** Osborn, J. A.; Jardine, F. H.; Young, J. F.; Wilkinson, G. *J. Chem. Soc. A* **1966**, 1711–1732.
- 16** Lee, I.-S.; Kwak, Y.-W.; Kim, D.-H.; Cho, Y.; Ohshita, J. *J. Organomet. Chem.* **2008**, *693*, 3233–3239.
- 17** Lu, P.; Lam, J. W. Y.; Liu, J.; Jim, C. K. W.; Yuan, W.; Chan, C. Y. K.; Xie, N.; Hu, Q.; Cheuk, K. K. L.; Tang, B. Z. *Macromolecules* **2011**, *44*, 5977–5986.
- 18** Berlman, I. B. *Handbook of Fluorescence Spectra of Aromatic Molecules*; Academic Press: New York and London, **1971**.
- 19** (a) Zhao, Z.; Lu, P.; Lam, J. W. Y.; Wang, Z.; Chan, C. Y. K.; Sung, H. H. Y.; Williams, I. D.; Ma, Y.; Tang, B. Z. *Chem. Sci.* **2011**, *2*, 672–675; (b) Zhao, Z.; Chen, S.; Deng, C.; Lam, J. W. Y.; Chan, C. Y. K.; Lu, P.; Wang, Z.; Hu, B.; Chen, X.; Lu, P.; Kwok, H. S.; Ma, Y.; Qiu, H.; Tang, B. Z. *J. Mater. Chem.* **2011**, *21*, 10949–10956.
- 20** (a) Akhavan, J. *The Chemistry of Explosives*; Royal Society of Chemistry: Cambridge, **2004**; (b) Peng, Y.; Zhang, A.-J.; Dong, M.; Wang, Y.-W. *Chem. Commun.* **2011**, *47*, 4505–4507.